Theoretical Study of the Structure, Bonding Nature, and Reductive Elimination Reaction of $Pd(XH_3)(\eta^3\text{-}C_3H_5)(PH_3)$ (X = C, Si, Ge, Sn). Hypervalent Behavior of Group 14 Elements

Bishajit Biswas, Manabu Sugimoto, and Shigeyoshi Sakaki*

Department of Applied Chemistry and Biochemistry, Faculty of Engineering, Kumamoto University, Kurokami, Kumamoto 860-8555, Japan

Received April 23, 1999

The structure and bonding nature of $Pd(XH_3)(\eta^3\text{-}C_3H_5)(PH_3)$ (**R-X**; X = C, Si, Ge, Sn) and its C−X reductive elimination were investigated with MP2-MP4(SDQ) and CCSD(T) methods. The C−C reductive elimination is considerably exothermic (27.7 kcal/mol) and needs a significantly large activation energy (23.0 kcal/mol), where CCSD(T) values are given hereafter. This considerably large exothermicity can be easily interpreted in terms of the strong C−C bond and the weak $Pd-CH_3$ bond. On the other hand, the C−Si, C−Ge, and C−Sn reductive eliminations easily occur with a moderate activation barrier (12−13 kcal/mol) and a moderate reaction energy; the exothermicities are 6.0 and 1.6 kcal/mol for the C−Si and C−Ge reductive eliminations, respectively, and the endothermicity of the C−Sn reductive elimination is 6.0 kcal/mol. These moderate reaction energies of C−Si, C−Ge, and C−Sn reductive eliminations are interpreted in terms of the decreasing orders of bond energy $E(C-C) > E(C-Si) > E(C-Ge) > E(C-Sn)$ and $E(Pd-SiH_3) > E(Pd-GeH_3) > E(Pd-SnH_3) \gg E(Pd-CH_3)$. The moderate activation barriers of C−Si, C−Ge, and C−Sn reductive eliminations are reflected in their transition state structures, in which SiH_3, GeH_3, and SnH_3 groups can interact with the allyl carbon atom, keeping the $Pd-SiH_3$, $Pd-GeH_3$, and $Pd-SnH_3$ bonds intact. These features result from the hypervalency of these elements. In the C−C reductive elimination, the $Pd-CH_3$ bond considerably weakens but the allyl$-CH_3$ bond is not completely formed at the TS, which is consistent with no hypervalency of the C atom. The η^1-allyl form, $Pd(XH_3)(\eta^1\text{-}C_3H_5)(PH_3)$, is much less stable than **R-X** by 7−8 kcal/mol. Intrinsic reaction coordinate calculations clearly show that the C−C reductive elimination occurs not through the η^1-allyl form but directly from $Pd(CH_3)(\eta^3\text{-}C_3H_5)(PH_3)$ if PH_3 does not exist in excess. If excess PH_3 exists in the reaction medium, the C−X reductive elimination via $Pd(XH_3)(\eta^1\text{-}C_3H_5)(PH_3)_2$ is not excluded. The $(\eta^3\text{-}C_3H_5)-XH_3$ (X = C, Sn) reductive elimination requires a larger activation energy than the CH_3-XH_3 reductive elimination, because the $Pd-(\eta^3\text{-}C_3H_5)$ bond is stronger than the $Pd-CH_3$ bond.

Downloaded by CARLI CONSORTIUM on June 30, 2009
Published on August 28, 1999 on http://pubs.acs.org | doi: 10.1021/om990296l

Introduction

Transition-metal η^3-allyl complexes including hydride, alkyl, silyl, and similar group 14 elements play versatile roles as active species and/or key intermediates in many organic transformations.[1] For instance, $PdH(\eta^3\text{-}C_3H_5)(PR_3)$ was postulated to serve as a key intermediate and to undergo C−H reductive elimination (eq 1) in Pd-

$$PdH(\eta^3\text{-}C_3H_5)(PR_3) \rightarrow Pd(CH_2{=}CHCH_3)(PR_3) \quad (1)$$

catalyzed reductive cleavage of allyl compounds by formic acid.[2−7] The same C−H reductive elimination was reported in η^3-allyl complexes of Ni and Pt.[8,9] The similar C−C reductive elimination of $M(aryl)(\eta^3\text{-}C_3H_5)(PR_3)_n$ (M = Ni, Pd; n = 1, 2) was investigated in detail.[10] $Pd(SiR_3)(\eta^3\text{-}C_3H_4\text{-}CH_2R)L_n$ was also proposed to play the

(1) For instance: (a) Chiusoli, G. P.; Salerno, G. In *The Chemistry of the Metal−Carbon Bond*; Hartley, F. R., Patai, S., Eds.; Wiley: Chichester, U.K., 1985; Vol. 3, Chapter 3.1, p 143. (b) Tsuji, J. In ref 1a, Chapter 3.2, p 163. (c) Sato, F. In ref 1a, Chapter 3.3, p 200. (d) Collman, J. P.; Hegedus, L. S.; Norton, J. R.; Finke, R. G. *Principles and Applications of Organotransition Metal Chemistry*; University Science Books: Mill Valley, CA, 1987; pp 175, 881. (e) Bäckvall, J.-E. In *Advances in Metal-Organic Chemistry*; Liebeskind, L. S., Ed.; JAI Press: Greenwich, CT, 1989; Vol. 1, p 135. (f) Hegedus, L. S. *Transition Metals in the Synthesis of Complex Organic Molecules*; University Science Books: Mill Valley, CA, 1994; p 261.

(2) Hey, H.; Arpe, H.-J. *Angew. Chem., Int. Ed. Engl.* **1973**, *12*, 928.

(3) (a) Tsuji, J.; Yamakawa, T. *Tetrahedron Lett.* **1979**, *7*, 613. (b) Tsuji, J.; Minami, I.; Shimizu, I. *Synthesis* **1986**, 623.

(4) Ono, N.; Hamamoto, I.; Kamimura, A.; Kaji, A. *J. Org. Chem.* **1986**, *57*, 3734.

(5) Ram, S.; Ehrenkauefer, A. *Synthesis* **1988**, 91.

(6) (a) Yamamoto, T.; Akimoto, M.; Saito, O.; Yamamoto, A. *J. Am. Chem. Soc.* **1981**, *103*, 9817. (b) Yamamoto, T.; Akimoto, M.; Saito, O.; Yamamoto, A. *Organometallics* **1986**, *5*, 1559. (c) Hayashi, T.; Yamamoto, A.; Hagihara, T. *J. Org. Chem.* **1986**, *51*, 723. (d) Oshima, M.; Shimizu, I.; Yamamoto, A.; Ozawa, F. *Organometallics* **1991**, *10*, 1221.

(7) Hayashi, T.; Iwamura, H.; Naito, M.; Matsumoto, Y.; Uozumi, Y.; Miki, M.; Yanagi, K. *J. Am. Chem. Soc.* **1994**, *116*, 775.

(8) Bonnemann, H. *Angew. Chem., Int. Ed. Engl.* **1970**, *9*, 736.

(9) Bertani, R.; Carturan, G.; Scrivanti, A. *Angew. Chem., Int. Ed. Engl.* **1983**, *22*, 246.

(10) (a) Kurosawa, H.; Emoto, M.; Ohnishi, H.; Miki, K.; Kasai, N.; Tatsumi, K.; Nakamura, A. *J. Am. Chem. Soc.* **1987**, *109*, 6333. (b) Kurosawa, H.; Ohnishi, H.; Emoto, M.; Kawasaki, Y.; Murai, S. *J. Am. Chem. Soc.* **1988**, *110*, 6272.

10.1021/om990296l CCC: $15.00 © 1999 American Chemical Society
Publication on Web 08/28/1999

role of key intermediate and to undergo the C−Si reductive elimination (eq 2) in Pd-catalyzed silylation

$$Pd(SiR_3)(\eta^3\text{-}C_3H_4\text{-}CH_2R)L_n \rightarrow Pd(RCH_2CH{=}CHCH_2SiR_3)L_n \quad (2)$$

of dienes[11,12] and allyl compounds.[13] The same type of C−Sn reductive elimination was reported in Pd(0)-catalyzed hydrostannation of dienes.[14] Interestingly, the reverse oxidative addition of allylstannane to Pd(0) (eq 3) was proposed recently in Pd-catalyzed carboxylation of allylstannanes[15] and Pd-catalyzed amine synthesis from allylstannanes.[16] Similar allylic C−C bond cleavage by Pd(0) (eq 4) was also thought to occur in Pd-catalyzed allylic alkylation.[17]

$$PdL_n + CH_2{=}CHCH_2SnR_3 \rightarrow Pd(SnR_3)(\eta^3\text{-}C_3H_5)L_n \quad (3)$$

$$PdL_n + CH_2{=}CHCH_2CH(CO_2Me)_2 \rightarrow Pd[CH(CO_2Me)_2](\eta^3\text{-}C_3H_5)L_n \quad (4)$$

It is of considerable interest that the reductive elimination of a Pd(II) η^3-allyl complex takes place in some reactions but the reverse oxidative addition of an allylic compound to Pd(0) takes place in other reactions. If we knew what allyl compound easily underwent the oxidative addition to Pd(0) to yield a Pd(II) η^3-allyl complex and what Pd(II) η^3-allyl complex easily underwent the reductive elimination to release an allyl compound, we would be able to present a reasonable design of organic transformation reactions with the Pd(II) η^3-allyl complex. Detailed knowledge of Pd(II) η^3-allyl complexes such as geometry, bonding nature, and reactivity is also useful and helpful for a good understanding of Pd-catalyzed organic transformation reactions.

In the past decade, several theoretical studies were carried out to investigate geometries and reactions of transition-metal η^3-allyl complexes. Some of them were semiempirical MO studies of the geometry of Pd(II) η^3-allyl complexes,[18] nucleophilic attack at the η^3-allyl ligand of Pd(II) complexes,[19,20] and C−C reductive elimination of a Pd(II) η^3-allyl methyl complex.[10a] Also, ab initio[21,22] and molecular mechanics[23] calculations were reported on geometries of Pd(II) and Ni(II) η^3-allyl complexes. Recently, ab initio studies were performed to investigate the C−H reductive elimination of MH(η^3-C_3H_5)(PH_3) (M = Pd, Pt)[24] and the nucleophilic attack at the η^3-allyl ligand.[25,26] Also, density functional studies were reported on the nucleophilic attack at the η^3-allyl ligand of Pd(II)[26,27] and the elimination of the Cl ligand from Pd(η^3-allyl)Cl(quinone).[28] However, no systematic investigation of the reductive elimination between η^3-allyl and group 14 elements (CH_3, SiH_3, GeH_3, and SnH_3) has yet been carried out. This type of systematic work would provide us with detailed information such as what Pd(II) η^3-allyl complex undergoes the reductive elimination to yield an organic allyl compound and what allyl compound undergoes the σ-bond cleavage by Pd(0) to yield a Pd(II) η^3-allyl complex.

Herein, we wish to report a systematic theoretical study of the geometry, bonding nature, and C−X reductive elimination (eq 5) of $Pd(XH_3)(\eta^3\text{-}C_3H_5)(PH_3)$ (X = C, Si, Ge, Sn) with MP2-MP4(SDQ) and CCSD(T) methods. In addition, we investigated the $\eta^3 \rightleftarrows \eta^1$

$$Pd(XH_3)(\eta^3\text{-}C_3H_5)(PH_3) \rightarrow Pd(\eta^2\text{-}C_3H_5\text{-}XH_3)(PH_3) \quad (5)$$

$$X = C, Si, Ge, Sn$$

interconversion of an allyl ligand (eq 6), since this interconversion was often reported to occur in many reactions[1] and the reductive elimination via an η^1-allyl species was discussed in detail in aryl−alkyl reductive elimination.[10]

$$Pd(XH_3)(\eta^3\text{-}C_3H_5)(PH_3) \rightarrow Pd(XH_3)(\eta^1\text{-}C_3H_5)(PH_3) \quad (6)$$

In this theoretical study, we hope to present detailed results of the geometries and bonding nature of Pd(XH_3)(η^3-C_3H_5)(PH_3), the reactivity difference of group 14 elements in the reductive elimination, the equilibrium between η^3-allyl and η^1-allyl complexes, and a comparison between the spontaneous reductive elimination from η^3-allyl species and the reductive elimination through η^3-allyl to η^1-allyl transformation.

Computational Details

Geometries of reactants, transition states, and products were optimized with the MP2 method, where the geometry of PH_3 was taken to be the same as the experimental structure of a free PH_3 molecule.[29] All transition state (TS) structures were determined so as to have only one negative eigenvalue of the Hessian matrix. Some of them were ascertained by

Downloaded by CARLI CONSORTIUM on June 30, 2009
Published on August 28, 1999 on http://pubs.acs.org | doi: 10.1021/om990296l

(11) Hayashi, T.; Hengrasmee, S.; Matsumoto, Y. *Chem. Lett.* **1990**, 1377.
(12) Obora, Y.; Tsuji, Y.; Kawamura, T. *J. Am. Chem. Soc.* **1993**, *115*, 10414; **1995**, *117*, 9814.
(13) Tsuji, Y.; Funato, M.; Ozawa, M.; Ogiyama, H.; Kajita, S.; Kawamura, T. *J. Org. Chem.* **1996**, *61*, 5779.
(14) Miyake, H.; Yamamura, K. *Chem. Lett.* **1992**, 1099.
(15) Shi, M.; Nicholas, K. M. *J. Am. Chem. Soc.* **1997**, *119*, 5057.
(16) Nakamura, H.; Nakamura, K.; Yamamoto, Y. *J. Am. Chem. Soc.* **1998**, *120*, 4242.
(17) Nilsson, Y. I. M.; Andersson, P. G.; Bäckvall, J.-E. *J. Am. Chem. Soc.* **1993**, *115*, 6609.
(18) Nakatsuji, K.; Yamaguchi, M.; Tatsumi, I.; Nakamura, A. *Organometallics* **1984**, *3*, 1257.
(19) Sakaki, S.; Nishikawa, M.; Ohyoshi, A. *J. Am. Chem. Soc.* **1980**, *102*, 4062.
(20) Curtis, M. D.; Eisenstein, O. *Organometallics* **1984**, *3*, 887.
(21) Goddard, R.; Krueger, C.; Mark, F.; Stansfield, R.; Zhang, X. *Organometallics* **1985**, *4*, 285.
(22) Szabo, K. J. *J. Am. Chem. Soc.* **1996**, *118*, 7818.
(23) (a) Norrby, P. O.; Åkermark, B.; Haeffner, F.; Hansen, S.; Blomberg, M. *J. Am. Chem. Soc.* **1993**, *115*, 4859. (b) Oslob, J. D.; Åkermark, B.; Helquist, P.; Norrby, P. O. *Organometallics* **1997**, *16*, 3015.
(24) Sakaki, S.; Satoh, H.; Shono, H.; Ujino, Y. *Organometallics* **1996**, *15*, 1713.
(25) Aranyos, A.; Szabo, K. J.; Castano, A. M.; Bäckvall, J.-E. *Organometallics* **1997**, *16*, 1058.
(26) Szabo, K. J.; Hupe, E.; Larsson, A. L. E. *Organometallics* **1997**, *16*, 3779.
(27) Gilardoni, F.; Weber, J.; Chermette, H.; Ward, T. R. *J. Phys. Chem. A* **1998**, *102*, 3607.
(28) Szabo, K. J. *Organometallics* **1998**, *17*, 1677.
(29) (a) Herzberg, G. *Molecular Spectra and Molecular Structure*; Van Nostrand: Princeton, NJ, 1967; Vol. 3, p 610. (b) We performed partial geometry optimization with the fixed geometry of PH_3, to save CPU time. The energy deviation by use of the fixed geometry of PH_3 is very small (Sakaki, S.; Satoh, H.; Shono, H.; Ujino, U. *Organometallics* **1996**, *15*, 1713). Since the optimized geometry of PH_3 deviates little from the experimental one used here, the frequency calculation could be carried out without any problem.

Downloaded by CARLI CONSORTIUM on June 30, 2009
Published on August 28, 1999 on http://pubs.acs.org | doi: 10.1021/om990296l

vibrational frequency calculations.[29b] Energy changes were calculated with MP2-MP4(SDQ) and CCSD (coupled cluster with single and double substitutions) methods, using the MP2-optimized geometries. In CCSD calculations, triple excitations were taken into consideration noniteratively.[30] Core orbitals were excluded from the active space in all calculations. These calculations were carried out with the Gaussian 94 program.[31] Energy changes calculated with the CCSD(T)/BS-II method are used for discussion, since this method is considered reliable for the compounds and reactions investigated here (see below).

Two kinds of basis set systems (BS-I and BS-II) were used. The smaller system (BS-I) was employed for geometry optimization, and the larger one (BS-II) was used for MP2-MP4-(SDQ) and CCSD(T) calculations. In BS-I, core electrons of Pd (up to 3d), P (up to 2p), Si (up to 2p), Ge (up to 3p), and Sn (up to 4p) were replaced with effective core potentials (ECPs).[32,33] Valence electrons of Pd were represented with a (311/311/31) set, and those of P, Si, Ge, and Sn were represented with (21/21/1) basis sets.[32,33] MIDI-3[34] and (31)[35] basis sets were used for C and H, respectively. In BS-II, the same ECPs as those in BS-I were employed for core electrons of Pd, P, Si, Ge, and Sn. Valence electrons of Pd were represented with a more flexible (311/311/211) set,[32] while valence electrons of P, Si, Ge, and Sn were represented with the same basis sets[33] as those of BS-I. A (721/41/1) basis set[35] was used for C.

Results and Discussion

Geometry of $Pd(XH_3)(\eta^3\text{-}C_3H_5)(PH_3)$ (X = C, Si, Ge, Sn) and Geometry Changes in the Reductive Elimination. Optimized geometries are shown in Figures 1 and 2. In all the reactants (**R-X**; X = C, Si, Ge, Sn), the $Pd-C^1$ bond at a position *trans* to PH_3 is shorter than the $Pd-C^3$ bond at a position *trans* to XH_3. The C^1-C^2 bond is longer than the C^2-C^3 bond in all the reactants. These geometrical features indicate that the η^3-allyl group moderately distorts toward an η^1-allyl structure. This is because methyl, silyl, germyl, and stannyl ligands exhibit stronger *trans* influence than PH_3. A similar distortion was reported theoretically in $MH(\eta^3\text{-}C_3H_5)(PH_3)$ (M = Pd, Pt)[24] and experimentally in $PdCl(\eta^3\text{-}C_3H_5)(PR_3)$;[36] in the former, the M−C bond positioned *trans* to hydride is longer than the other M−C bond and the C−C bond positioned *trans* to hydride is shorter than the other C−C bond. In the latter, the Pd−C bond positioned *trans* to PR_3 is longer than the other M−C bond and the C−C bond positioned *trans* to PR_3 is shorter than the other C−C bond. These results were also interpreted in terms that hydride and PR_3 exhibit stronger *trans* influence than phosphine and Cl, respectively. Although the distortion toward the η^1-allyl structure occurs in **R-X**, the C^1-C^2 distance is shorter and the C^2-C^3 distance is longer than the C−C single bond (1.540 Å) and the C=C double bond (1.340 Å) of propene, respectively. These geometrical features indicate that the C^1-C^2 bond conjugates well with the C^2-C^3 bond and that the allyl group is still considered an η^3-allyl ligand in $Pd(XH_3)(\eta^3\text{-}C_3H_5)(PH_3)$, like that in $MH(\eta^3\text{-}C_3H_5)(PH_3)$ (M = Pd, Pt).[24] It is also noted that the *trans* influence of group 14 elements increases in the order $CH_3 \ll GeH_3 < SnH_3 \approx SiH_3$ since the $Pd-C^3$ bond at a position *trans* to XH_3 becomes longer in the order $CH_3 \ll GeH_3 < SnH_3 \approx SiH_3$ (Figures 1 and 2).

In all the transition states (**TS-X**; X = C, Si, Ge, Sn), the $Pd-C^1$ and Pd−X bond distances lengthen and the $Pd-PH_3$ bond distance shortens, compared to those in **R-X**. To form the C^1-XH_3 bond, XH_3 must approach C^1, which causes the $Pd-C^1$ bond weakening. Consequently, the *trans* influence of the C^1 atom weakens, and therefore, the $Pd-PH_3$ distance shortens at the TS since PH_3 is at a position *trans* to C^1. It should be also noted that although the C^2-C^3 bond lengthens little in all the transition states, the C^1-C^2 bond somewhat lengthens by 0.05 Å in the transition states except for **TS-C** of the C−C reductive elimination in which the C^1-C^2 bond lengthens by 0.03 Å. As a result, the allyl moiety of **TS-Si**, **TS-Ge**, and **TS-Sn** resembles propene well. In **TS-C**, on the other hand, the geometry of the allyl group is intermediate between those of reactant and product. Consistent with the above differences between the CH_3 reaction system and the others, the C^1-CH_3 distance of **TS-C** is much longer than that of the product **Prd-C** by 0.55 Å, while the C^1-Si, C^1-Ge, and C^1-Sn distances at the TS are only 0.16−0.20 Å longer than those of the product. Also, the $Pd-CH_3$ distance lengthens greatly by 0.27 Å, while the $Pd-SiH_3$, $Pd-GeH_3$, and $Pd-SnH_3$ distances lengthen to a lesser extent than does the $Pd-CH_3$ bond. These results suggest that (1) the $Pd-CH_3$ bond weakens very much in **TS-C**, while the C^1-CH_3 bond formation is underway, and that (2) the $Pd-SiH_3$, $Pd-GeH_3$, and $Pd-SnH_3$ bonds are not weakened very much,[37] while the C−Si, C−Ge, and C−Sn bond formation is about 70−80% completed at the TS.[38] In other words, SiH_3, GeH_3, and SnH_3 groups can form a new bonding interaction with the allyl carbon atom, keeping the $Pd-SiH_3$, $Pd-GeH_3$, and $Pd-SnH_3$ bonds intact, unlike the CH_3 group. This feature of Si, Ge, and Sn elements is related to the hypervalency. Actually, these transition states can be considered to take a distorted-trigonal-bipyramidal

(30) Pople, J. A.; Head-Gordon, M.; Raghavachari, K. *J. Chem. Phys.* **1987**, *87*, 5968.
(31) Frisch, M. J.; Trucks, G. W.; Schlegel, H. B.; Gill, P. M. W.; Johnson, B. G.; Robb, M. A.; Cheeseman, J. R.; Keith, T. A.; Petersson, G. A.; Montgomery, J. A.; Raghavachari, K.; Al-Laham, M. A.; Zakrzewski, V. G.; Ortiz, J. V.; Foresman, J. B.; Cioslowski, J.; Stefanov, B. B.; Nanayakkara, A.; Challacombe, M.; Peng, C. Y.; Ayala, P. Y.; Chen, W.; Wong, M. W.; Andres, J. L.; Replogle, E. S.; Gomperts, R.; Martin, R. L.; Fox, D. J.; Binkley, J. S.; DeFrees, D. J.; Baker, J.; Stewart, J. J. P.; Head-Gordon, M.; Gonzalez, C.; Pople, J. A. Gaussian 94; Gaussian Inc., Pittsburgh, PA, 1994.
(32) Hay, P. J.; Wadt, W. R. *J. Chem. Phys.* **1985**, *82*, 299.
(33) Wadt, W. R.; Hay, P. J. *J. Chem. Phys.* **1985**, *82*, 284.
(34) Huzinaga, S.; Andzelm, J.; Klobukowski, M.; Radizo-Andzelm, E.; Sakai, Y.; Tatewaki, H. *Gaussian Basis Sets for Molecular Calculations*; Elsevier: Amsterdam, 1984.
(35) Dunning, T. H.; Hay, P. J. In *Methods of Electronic Structure Theory*; Schaeffer, H. F., Ed.; Plenum: New York, 1977: Vol. 4, p 1.
(36) Mason, R.; Russell, D. R. *Chem. Commun.* **1966**, 26. (b) Smith, A. E. *Acta Crystallogr.* **1969**, *A25*, 5161.

(37) $Pd-SiH_3$, $Pd-GeH_3$, and $Pd-SnH_3$ bond distances are 2.497, 2.624, and 2.830 Å in **TS-Si**, **TS-Ge**, and **TS-Sn**, respectively, which are 0.13, 0.18, and 0.22 Å longer than those in the reactant. However, the $Pd-CH_3$ bond is 2.408 Å, which is 0.27 Å longer than that in the reactant. When $Pd-CH_3$, $Pd-SiH_3$, $Pd-GeH_3$, and $Pd-SnH_3$ bonds are lengthened as those in the TS with the other part fixed, the destabilization energy is 19.0, 10.3, 11.2, and 12.0 kcal/mol for X = C, Si, Ge, and Sn, respectively. These are about 25% of the $Pd-SiH_3$, $Pd-GeH_3$, and $Pd-SnH_3$ bond energies but 73% of the $Pd-CH_3$ bond energy.

(38) In $CH_2{=}CHCH_2XH_3$, the C−C, C−Si, C−Ge, and C−Sn bond distances are 1.557, 1.908, 1.997, and 2.174 Å, respectively. In **TS-C**, **TS-Si**, **TS-Ge**, and **TS-Sn**, these bond distances are 2.112, 2.189, 2.249, and 2.355 Å, respectively. The difference in energy of $CH_2{=}CHCH_2XH_3$ between the distorted geometry taken in the TS and the equilibrium structure was calculated to be 52.5, 22.5, 17.3, and 9.6 kcal/mol for X = C, Si, Ge, and Sn, respectively. These are about 58%, 26%, 22%, and 14% of the C−C, C−Si, C−Ge, and C−Sn bond energies, respectively. Thus, the C−Si, C−Ge, and C−Sn bond formations are about 80% completed at the TS, while the C−C bond formation is not completed at all.

Downloaded by CARLI CONSORTIUM on June 30, 2009
Published on August 28, 1999 on http://pubs.acs.org | doi: 10.1021/om990296l

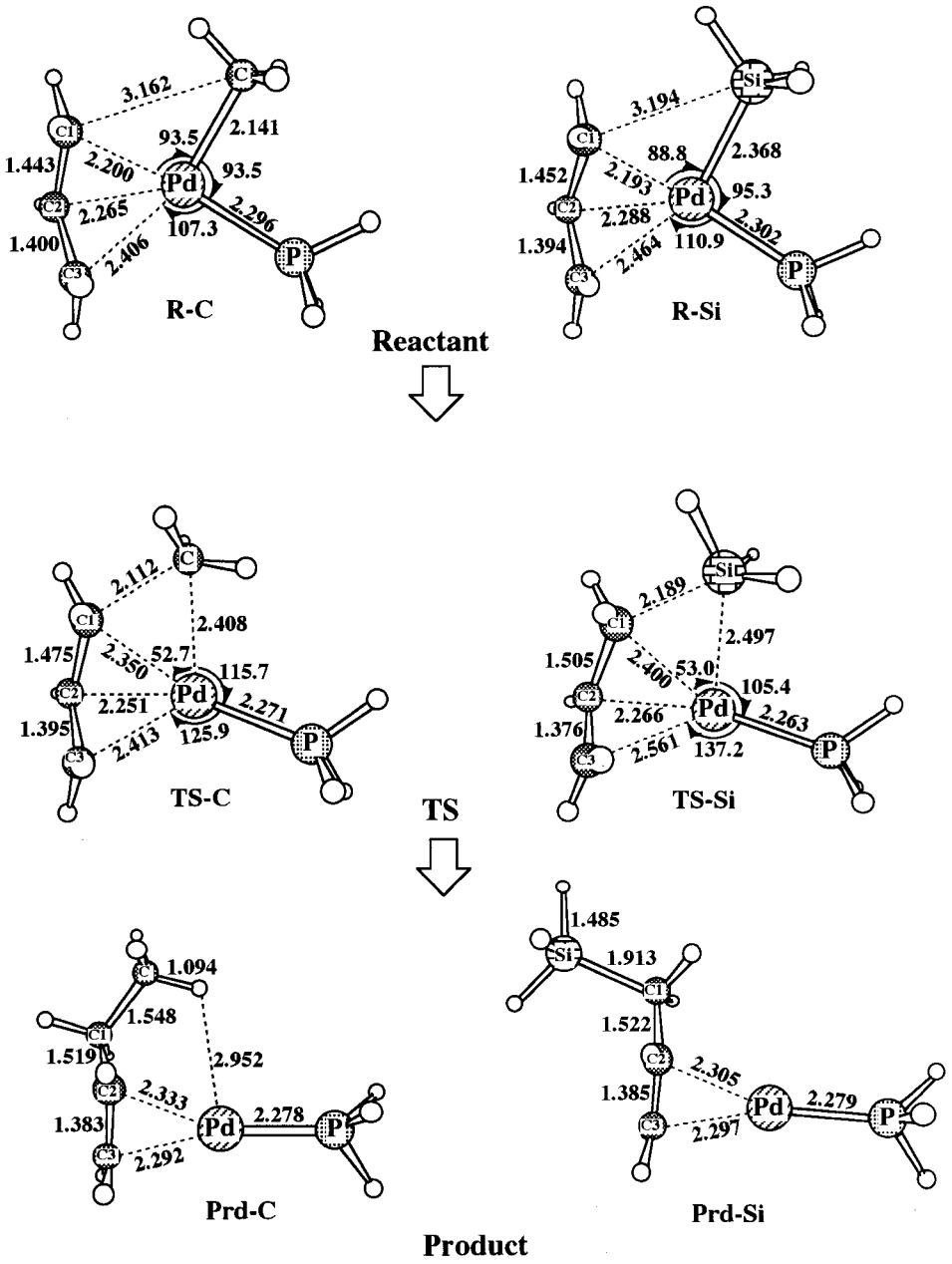

Figure 1. Geometry changes in the C−C and C−Si reductive eliminations of $Pd(CH_3)(\eta^3\text{-}C_3H_5)(PH_3)$ and $Pd(SiH_3)(\eta^3\text{-}C_3H_5)(PH_3)$, respectively. Bond lengths are in Å, and bond angles are in deg.

structure around these elements, as shown in Scheme 1, since the Pd−XH_3 bond is kept and the C^1−XH_3 bond formation is 70−80% completed. As a result, the C−Si, C−Ge, and C−Sn reductive eliminations can take place with a moderate activation barrier, as will be discussed below.

The product (**Prd-X**; X = C, Si, Ge, or Sn) is a palladium(0) alkene complex, in which the C=C double bond is 0.05 Å longer than that of free propene derivatives, CH_2=$CHCH_2XH_3$, as expected. The C^2=C^3, Pd−C^2, and Pd−C^3 distances depend little on the kind of XH_3 species. XH_3 takes a suitable position to minimize the steric repulsion between XH_3 and Pd in **Prd-Si**, **Prd-Ge**, and **Prd-Sn**.[39] This is because Pd(0) cannot form an agostic interaction with XH_3 but gives rise to steric repulsion with XH_3 due to the d^{10} electron configuration of Pd(0) (remember that the empty d orbital is necessary for the agostic interaction).[40] However, the geometry of 1-butene in $Pd(CH_2$=$CHC_2H_5)(PH_3)$ (**Prd-C**) is different from the others, while a very

(39) (a) There are three minima in the geometry of **Prd-X**; in the first, XH_3 takes the most distant position from Pd as in **Prd-Si**, **Prd-Ge** and **Prd-Sn**, and in the second, XH_3 takes the nearest position to Pd as in **Prd-C**. The third is somewhat less stable than the first and second isomers, and therefore, it is not mentioned here. The energy difference between the first and the second minima is very small; the former is more stable than the latter by −0.2, 0.2, 0.5, and 0.1 kcal/mol for X = C, Si, Ge, Sn, respectively, at the CCSD(T)/BS-II level, where the negative value represents that the former is less stable. The rotation barrier is calculated to be 4.5 kcal/mol for X = C and 4.0 kcal/mol for X = Si with the MP2/BS-II method. (b) To estimate the steric repulsion between XH_3 and PH_3, an energy difference was calculated between these two minima where Pd was eliminated from the system. Only a negligibly small energy difference was observed. Thus, the steric repulsion between XH_3 and PH_3 is not responsible for the result that SiH_3, GeH_3, and SnH_3 take a position distant from Pd unlike CH_3 in **Prd-X**. Not PH_3 but the d^{10} electron configuration of Pd would give rise to a steric repulsion with SiH_3, GeH_3, and SnH_3 greater than that with CH_3 because SiH_3, GeH_3, and SnH_3 can take a position closer to Pd than CH_3 due to the C−Si, C−Ge, and C−Sn bonds being longer than the C−C bond.

Downloaded by CARLI CONSORTIUM on June 30, 2009
Published on August 28, 1999 on http://pubs.acs.org | doi: 10.1021/om990296l

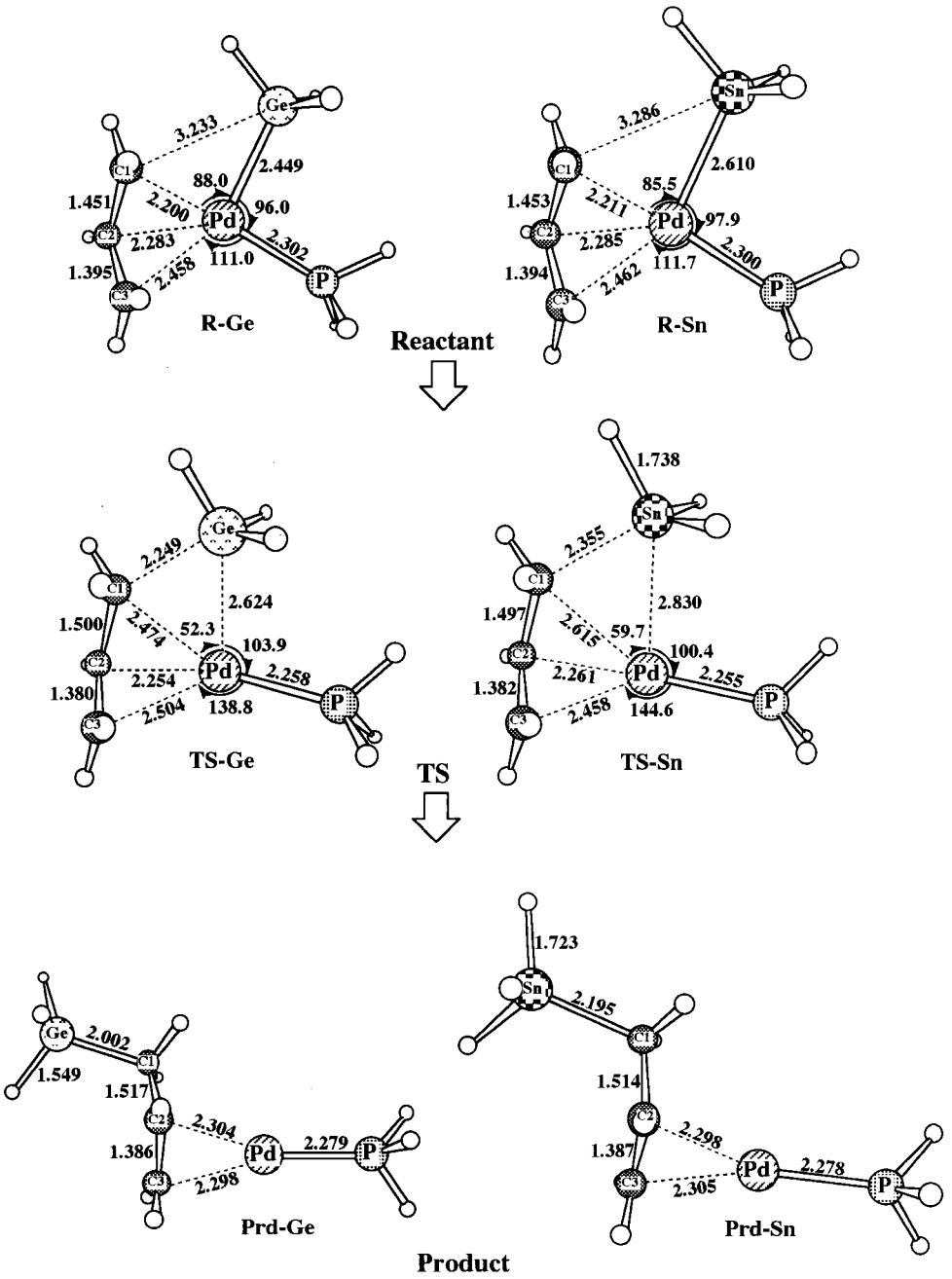

Figure 2. Geometry changes in the C−Ge and C−Sn reductive eliminations of $Pd(GeH_3)(\eta^3\text{-}C_3H_5)(PH_3)$ and $Pd(SnH_3)(\eta^3\text{-}C_3H_5)(PH_3)$, respectively. Bond lengths are in Å, and bond angles are in deg.

small energy increase (only 0.2 kcal/mol) occurs even when 1-butene takes the same conformation as that in **Prd-Si**, **Prd-Ge**, and **Prd-Sn**. The agostic interaction between Pd and the CH_3 group is not formed, as discussed above. Actually, the H atom of CH_3 is quite distant from Pd and all three C−H bond distances are normal. The reason **Prd-C** takes this structure is not clear at this moment.

Frequency Analysis of the Transition State. All these transition state structures were examined with vibrational frequency calculations. In **TS-C**, only one imaginary frequency of 419*i* cm^{-1} is observed, indicating

Scheme 1

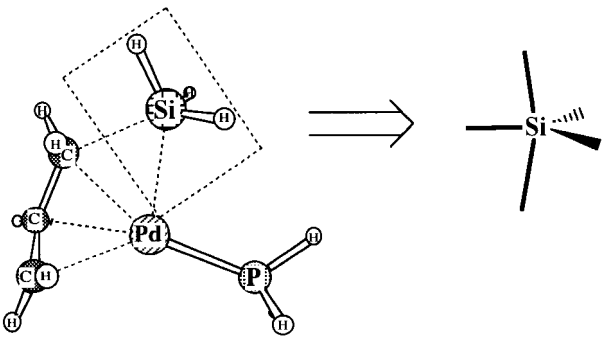

that this is a true TS. The eigenvector of this frequency indicates that the CH_3 group is changing its direction toward the C^1 atom, and at the same time, the C^1 atom

(40) (a) Koga, N.; Obara, S.; Morokuma, K. *J. Am. Chem. Soc.* **1984**, *106*, 4625. (b) Obara, S.; Koga, N.; Morokuma, K. *J. Organomet. Chem.* **1984**, *270*, C38. (c) Koga, N.; Morokuma, K. *J. Am. Chem. Soc.* **1988**, *110*, 0, 108.

Table 1. Activation Barrier E_a[a] and Reaction Energy ΔE[b] of the C−X Reductive Elimination of $Pd(XH_3)(\eta^3\text{-}C_3H_5)(PH_3)$ (X = C, Si, Ge, Sn)[c]

	CH_3		SiH_3		GeH_3		SnH_3	
	E_a	ΔE	E_a	ΔE	E_a	ΔE	E_a	ΔE
MP2	22.1	−26.1	13.0	−4.0	14.4	0.6	13.8	8.4
MP3	25.7	−30.6	11.6	−9.1	12.6	−4.6	10.5	2.8
MP4(DQ)	22.6	−31.6	11.5	−7.8	12.7	−3.2	11.5	4.7
MP4(SDQ)	18.9	−32.4	9.7	−8.2	11.0	−3.7	10.3	4.4
CCSD	24.3	−30.1	11.4	−8.2	12.6	−3.7	10.9	3.8
CCSD(T)	23.3	−27.7	11.6	−6.0	12.8	−1.6	11.5	5.9

[a] $E_a = E_t(TS) - E_t(reactant)$. [b] $\Delta E = E_t(product) - E_t(reactant)$. [c] In kcal/mol. BS-II was used.

approaches CH_3. These geometry changes correspond to the Pd−CH_3 bond breaking and the C^1−CH_3 bond formation. Thus, this eigenvector is consistent with the geometry changes of the C−C reductive elimination. **TS-Si**, **TS-Ge**, and **TS-Sn** exhibit also only one imaginary frequency, 207*i*, 175*i*, and 133*i* cm^{-1}, respectively, in which similar geometry changes occur. It should be noted that **TS-C** exhibits the greatest imaginary frequency, and the imaginary frequency value decreases in the order **TS-C** ≫ **TS-Si** > **TS-Ge** > **TS-Sn**. Since this frequency is directly related to the curvature of the potential energy surface at the TS, the potential energy curve of the C−C reductive elimination is considered the steepest at the TS and that of the C−Sn reductive elimination is the smoothest. These differences would be related to the E_a value, as will be discussed below.

Energy Changes by Reductive Elimination. The activation barrier (E_a) and the reaction energy (ΔE) were calculated with MP2-MP4(SDQ) and CCSD(T) methods, where E_a is defined as an energy difference between TS and the reactant and ΔE is an energy difference between the product and the reactant. As shown in Table 1, E_a and ΔE values only slightly fluctuate upon going to CCSD(T) from MP4SDQ. Thus, it is reasonably concluded that CCSD(T) values are reliable in investigating these reductive elimination reactions, and therefore, energy changes calculated with the CCSD(T)/BS-II method are given from now on.

Several interesting results observed in Table 1 can be summarized as follows. (1) The C−C reductive elimination of $Pd(CH_3)(\eta^3\text{-}C_3H_5)(PH_3)$ is significantly exothermic (E_{exo} = 27.7 kcal/mol) and requires a considerably large E_a value of 23.3 kcal/mol. The large E_a value is consistent with the large imaginary frequency value of **TS-C**. (2) On the other hand, the C−Si and C−Ge reductive eliminations of $Pd(SiH_3)(\eta^3\text{-}C_3H_5)(PH_3)$ and $Pd(GeH_3)(\eta^3\text{-}C_3H_5)(PH_3)$ proceed with moderate E_a values of 11.6 and 12.8 kcal/mol, respectively, and small exothermicities of 6.0 and 1.6 kcal/mol, respectively. (3) The C−Sn reductive elimination of $Pd(SnH_3)(\eta^3\text{-}C_3H_5)(PH_3)$ also proceeds with a moderate E_a value of 11.5 kcal/mol and small endothermicity (E_{endo} = 5.9 kcal/mol). This small endothermicity is consistent with the experimental results that the oxidative addition of allylstannane occurs under some reaction conditions while the reductive elimination takes place under different conditions. Considering that the C−Si and C−Ge reductive eliminations are only slightly exothermic, one might expect that allylsilane and allylgermane undergo both oxidative addition and reductive elimination like allylstannane, depending on the reaction conditions.

Scheme 2

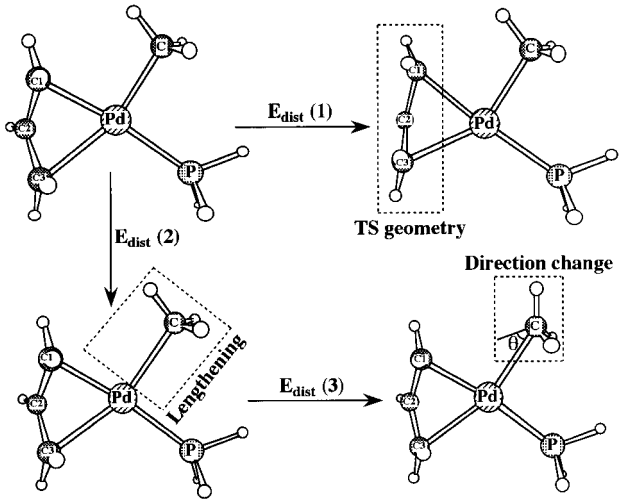

Table 2. Distortion Energies (kcal/mol)[a] in the Transition State

XH_3	$E_{dist}(1)$[b]	$E_{dist}(2)$[c]	$E_{dist}(3)$[d]
CH_3	2.6	7.3	22.0
SiH_3	6.4	1.2	13.8
GeH_3	6.0	2.0	11.7
SnH_3	6.0	2.9	11.1

[a] The CCSD(T) calculation with BS-II. [b] A destabilization energy by the distortion of the allyl part like that in the TS. [c] A destabilization energy by the Pd−XH_3 bond lengthening like that in the TS. [d] A destabilization energy by the direction change of XH_3 like that in the TS.

Why is the Activation Barrier the Highest in the C−C Reductive Elimination of $Pd(CH_3)(\eta^3\text{-}C_3H_5)(PH_3)$? To find the reason that the C−C reductive elimination needs a very large activation energy, we calculated first the distortion energy $E_{dist}(1)$ of the allyl part, in which only the allyl part was assumed to take the distorted geometry in the TS (see Scheme 2). As shown in Table 2, the $E_{dist}(1)$ value of **TS-C** is similar to those of the others; the difference is only 3−6 kcal/mol. Then, we calculated the distortion energy $E_{dist}(2)$ caused by the Pd−XH_3 bond lengthening and the distortion energy $E_{dist}(3)$ caused by the direction change of XH_3, in which the Pd−XH_3 bond was lengthened to the distance in the TS and the direction of XH_3 was changed as that in the TS with the other part fixed, as shown in Scheme 2. Both $E_{dist}(2)$ and $E_{dist}(3)$ of **TS-C** are much larger than those of **TS-Si**, **TS-Ge**, and **TS-Sn**. Moreover, the difference in E_a between CH_3 and the other reaction systems is not very different from the difference in the sum of $E_{dist}(2)$ and $E_{dist}(3)$ between CH_3 and the other systems. From these results, it should be reasonably concluded that the large distortion energy of the Pd−CH_3 bond is responsible for the large E_a value of the CH_3 reaction system.

In particular, it is noted that $E_{dist}(3)$ of the CH_3 system is much larger than that of the others. This means that the direction of the CH_3 group changes with great difficulty but the direction of SiH_3, GeH_3, and SnH_3 groups easily changes with a much smaller destabilization energy. In other words, SiH_3, GeH_3, and SnH_3 groups can shift their directions from Pd without a large destabilization energy. This feature is consistent with the hypervalency of these elements.

Downloaded by CARLI CONSORTIUM on June 30, 2009
Published on August 28, 1999 on http://pubs.acs.org | doi: 10.1021/om990296l

Table 3. C−XH_3 and Pd−XH_3 Bond Energies (X = C, Si, Ge, Sn)[a]

system	bond energy	MP2	MP3	MP4(DQ)	MP4(SDQ)	CCSD	CCSD(T)
CH_3-CH_3	E(C−C)	98.6	95.2	94.0	94.3	93.5	95.3
CH_3-SiH_3	E(C−Si)	89.1	87.0	85.9	86.1	85.4	86.7
CH_3-GeH_3	E(C−Ge)	81.2	78.8	77.7	77.9	77.3	78.6
CH_3-SnH_3	E(C−Sn)	71.5	70.0	68.0	68.2	67.5	68.9
cis-$PdH_2(PH_3)_2$	E(Pd−H)	50.9	51.6	52.7	53.3	52.6	52.8
cis-$Pd(H)(CH_3)(PH_3)_2$	E(Pd−CH_3)	27.4	25.0	23.3	22.5	24.2	26.3
cis-$Pd(H)(SiH_3)(PH_3)_2$	E(Pd−SiH_3)	45.6	42.4	43.7	45.0	42.9	44.5
cis-$Pd(H)(GeH_3)(PH_3)_2$	E(Pd−GeH_3)	40.3	36.7	38.1	38.8	37.0	38.6
cis-$Pd(H)(SnH_3)(PH_3)_2$	E(Pd−SnH_3)	39.3	35.7	37.3	37.7	36.0	37.5

[a] In kcal/mol. BS-II was used.

Reaction Energy and Pd−XH_3 and C−X Bond Energies (X = C, Si, Ge, Sn). As mentioned above, the C−X reductive elimination of $Pd(XH_3)(\eta^3\text{-}C_3H_5)(PH_3)$ becomes more exothermic in the order C−Sn < C−Ge < C−Si ≪ C−C. This result can be explained in terms of C−XH_3 and Pd−XH_3 bond energies.

The C−XH_3 bond energy was estimated by considering the reaction

$$CH_3-XH_3 \rightarrow {}^{\bullet}CH_3 + {}^{\bullet}XH_3 \qquad (7)$$

The Pd−H bond energy was estimated with eqs 8a and 8b. The sum of Pd−H and Pd−XH_3 bond energies was calculated with eqs 9a−d, and then the Pd−XH_3 bond energy was evaluated by subtracting the Pd−H bond energy from the sum.

$$H_2 \rightarrow 2{}^{\bullet}H \qquad (8a)$$

$$Pd(PH_3)_2 + H_2 \rightarrow \textit{cis}\text{-}PdH_2(PH_3)_2 \qquad (8b)$$

$$Pd(PH_3)_2 + CH_4 \rightarrow \textit{cis}\text{-}Pd(H)(CH_3)(PH_3)_2 \qquad (9a)$$

$$Pd(PH_3)_2 + SiH_4 \rightarrow \textit{cis}\text{-}Pd(H)(SiH_3)(PH_3)_2 \qquad (9b)$$

$$Pd(PH_3)_2 + GeH_4 \rightarrow \textit{cis}\text{-}Pd(H)(GeH_3)(PH_3)_2 \qquad (9c)$$

$$Pd(PH_3)_2 + SnH_4 \rightarrow \textit{cis}\text{-}Pd(H)(SnH_3)(PH_3)_2 \qquad (9d)$$

As shown in Table 3, those values little depend on the computational methods, indicating that these bond energies are reliably calculated here. The C−XH_3 bond energy increases in the order E(C−Sn) < E(C−Ge) < E(C−Si) < E(C−C), and the Pd−XH_3 bond energy increases in the order E(Pd−CH_3) ≪ E(Pd−SnH_3) < E(Pd−GeH_3) < E(Pd−SiH_3). The greatest exothermicity of the C−C reductive elimination arises from the fact that the Pd−CH_3 bond is the weakest but the C−C bond is the strongest. In the C−Sn reductive elimination, the next weakest Pd−SnH_3 bond is broken but the next weakest C−Sn bond is formed. In the C−Si reductive elimination, the strongest Pd−SiH_3 bond is broken and the second strongest C−Si bond is formed. The C−Ge reductive elimination is in the intermediate situation between the C−Si and C−Sn reductive eliminations. As a result, these reductive eliminations are either slightly exothermic or slightly endothermic.

The next issue to be discussed is the reason that the Pd−CH_3 bond is much weaker than the Pd−SiH_3, Pd−GeH_3, and Pd−SnH_3 bonds. According to simple molecular orbital considerations, the stabilization energy $\Delta\epsilon_t$ from covalent bond formation can be represented as

Table 4. Overlap Integrals between Pd and the SOMO (sp^3 Radical Orbital) of XH_3[a] (X = C, Si, Ge, Sn)

	$\langle\phi_{sp^3}\|\phi_{5s}\rangle$	$\langle\phi_{sp^3}\|\phi_{5p_z}\rangle$	$\langle\phi_{sp^3}\|\phi_{4d_{z^2}}\rangle$
Pd−CH_3	0.1351	0.1528	0.2764
Pd−SiH_3	0.1605	0.4512	0.3452
Pd−GeH_3	0.1374	0.4495	0.3116
Pd−SnH_3	0.1200	0.4790	0.2795

[a] r(Pd−C) = 2.107 Å, r(Pd−Si) = 2.389 Å, r(Pd−Ge) = 2.513 Å, and r(Pd−Sn) = 2.737 Å; BS-II was used.

$$\Delta\epsilon_t = \alpha_A - \alpha_B + \frac{2\beta^2}{\alpha_A - \alpha_B} \qquad (10)$$

where α_A and α_B represent the d orbital energy of a metal part and the SOMO (singly occupied molecular orbital; i.e., sp^3 radical orbital) energy of an XH_3 radical, respectively, and β is a resonance integral. This equation means that the bond stabilization energy increases with an increase in $\alpha_A - \alpha_B$ when β is small. Considering eq 10, we could successfully explain the fact that the Pd−alkyl bond becomes strong by introducing an electron-withdrawing substituent on the sp^3 C atom.[41] The SOMO energy is calculated here to be −10.4, −9.2, −9.0, and −8.6 eV for CH_3, SiH_3, GeH_3, and SnH_3, respectively, where BS-II was used.[42] However, the decreasing order of bond energy Pd−SiH_3 > Pd−GeH_3 > Pd−SnH_3 ≫ Pd−CH_3 cannot be explained in the same way, as follows. If we considered the orbital energy, the Pd−CH_3 bond was the strongest because the SOMO of CH_3 lies at the lowest energy. Therefore, other factors should be taken into consideration. The β value is one of the plausible factors to be considered. Actually, the β value of Pd−CH_3 is considered to be smaller than that of the others, since the overlap integral between Pd and CH_3 is much smaller than that between Pd and SiH_3, GeH_3, or SnH_3, as shown in Table 4. From this factor, the Pd−CH_3 bond is much weaker than the others despite the fact that the SOMO of CH_3 is at a very low energy.

The decreasing order of bond energy Pd−SiH_3 > Pd−GeH_3 > Pd−SnH_3 is also an interesting and important

(41) Sakaki, S.; Biswas, B.; Sugimoto, M. *Organometallics* **1998**, *17*, 1278.

(42) (a) The IP values of these neutral radicals are calculated to be 10.45, 9.23, 8.96, and 8.48 eV with the CCSD(T)/BS-II method. These IP values are parallel to the SOMO energy level, indicating that the SOMO energy level can be used as a measure of the energy level of sp^3 electrons. Also, the calculated IP values agree well with the recently reported values.[42b] (b) Curtiss, L. A.; Raghavachari, K.; Redferm, P. C.; Rassolov, V.; Pople, J. A. *J. Chem. Phys.* **1998**, *109*, 7764 and references therein.

Downloaded by CARLI CONSORTIUM on June 30, 2009
Published on August 28, 1999 on http://pubs.acs.org | doi: 10.1021/om990296l

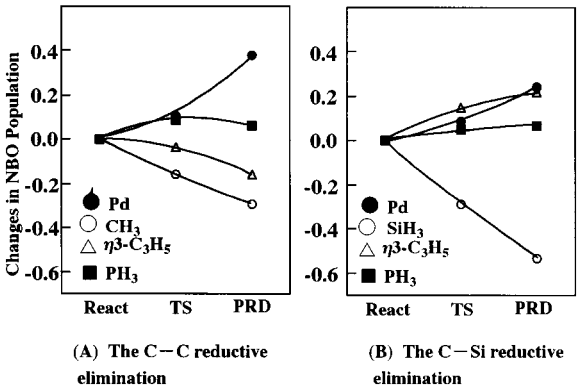

Figure 3. Natural bond orbital population changes in the C−C and C−Si reductive elimination of $Pd(CH_3)(\eta^3\text{-}C_3H_5)(PH_3)$ and $Pd(SiH_3)(\eta^3\text{-}C_3H_5)(PH_3)$, respectively. A positive value represents an increase in population (and vice versa).

result. Since the SOMO energy decreases in the order $SnH_3 > GeH_3 > SiH_3$, the $\alpha_A - \alpha_B$ term decreases in this order, which leads to the increasing order of bond energy $Pd-SnH_3 < Pd-GeH_3 < Pd-SiH_3$. The other factor to be considered is β. As shown in Table 4, the overlap integral between Pd and the SOMO of XH_3 decreases in the order $Pd-SiH_3 > Pd-GeH_3 > Pd-SnH_3$. This is also responsible for the decreasing order of bond energy $Pd-SiH_3 > Pd-GeH_3 > Pd-SnH_3$.

Population Changes in the Reductive Elimination. Electron distribution is examined with natural bond orbital population.[43] Electron populations of allyl and CH_3 decrease, those of Pd and PH_3 increase, and Pd d orbital population considerably increases in the C−C reductive elimination of $Pd(CH_3)(\eta^3\text{-}C_3H_5)(PH_3)$, as shown in Figure 3. These changes are consistent with the understanding that this is a reductive elimination reaction. In the C−Si, C−Ge, and C−Sn reductive eliminations, on the other hand, slightly different population changes are observed; electron populations of SiH_3, GeH_3, and SnH_3 decrease to a greater extent than that of CH_3, while Pd atomic population increases to a lesser extent than that in the C−C reductive elimination and the allyl electron population increases surprisingly (in Figure 3, population changes of C−Ge and C−Sn reductive eliminations are omitted to save space, since they are almost the same as that of the C−Si reductive elimination). The increase of allyl electron population is not consistent with our understanding that these reactions are reductive eliminations.

We can easily understand these population changes by inspecting the electron distribution of reactants. In $Pd(CH_3)(\eta^3\text{-}C_3H_5)(PH_3)$ (**R-C**), the Pd atomic population is much smaller but the CH_3 electron population is much greater than those in the others, as shown in Table 5. These are because CH_3 is more electron-withdrawing than SiH_3, GeH_3, and SnH_3. Since the Pd atomic population is insufficient in **R-C** due to the large electronegativity of CH_3, the Pd atomic population must increase considerably in the C−C reductive elimination but increases to a lesser extent in the C−Si, C−Ge, and C−Sn reductive eliminations than does that in the C−C reductive elimination (Figure 3). On the other hand, the electron population of the allyl group is hardly different in **R-X**, while populations of SiH_3, GeH_3, and SnH_3 are much smaller than that of CH_3. These results indicate that although SiH_3, GeH_3, and SnH_3 are more electron-donating to Pd(II) than is CH_3 the electron donation from η^3-allyl to Pd is little influenced by XH_3. Nevertheless, the allyl population increases but the XH_3 population decreases greatly in the C−Si, C−Ge, and C−Sn reductive eliminations. These results suggest that the η^3-allyl ligand is strongly electron-donating to Pd(II) but the η^1-allyl group tends to receive electrons from SiH_3, GeH_3, and SnH_3 because of the electronegativity difference between Si, Ge, Sn, and C and that the charge transfer from SiH_3, GeH_3, and SnH_3 to η^1-allyl occurs to a considerable extent in the reductive elimination. From the above discussion, the C−Si, C−Ge, and C−Sn reductive eliminations are reasonably characterized as intramolecular nucleophilic attacks of SiH_3, GeH_3, and SnH_3 at the η^3-allyl ligand.

Table 5. Electron Distribution[a] and Relative Stabilities (ΔE)[b] of $Pd(XH_3)(\eta^3\text{-}C_3H_5)(PH_3)$, $Pd(XH_3)(\eta^1\text{-}C_3H_5)(PH_3)$, and $Pd(XH_3)(\eta^1\text{-}C_3H_5)(PH_3)_2$

	XH_3			
	CH_3	SiH_3	GeH_3	SnH_3
(A) $Pd(XH_3)(\eta^3\text{-}C_3H_5)(PH_3)$				
Pd	45.736	45.864	45.869	45.891
XH_3	9.275	17.145	35.144	53.096
$\eta^3\text{-}C_3H_5$	23.196	23.204	23.197	23.215
PH_3	17.792	17.787	17.791	17.797
(B) $Pd(XH_3)(\eta^1\text{-}C_3H_5)(PH_3)$				
ΔE_1[b,c]	8.6	7.2	7.6	7.8
Pd	45.746	45.882	45.889	45.913
XH_3	9.174	17.044	35.038	52.990
$\eta^1\text{-}C_3H_5$	23.228	23.249	23.246	23.266
PH_3	17.852	17.825	17.829	17.831
(C) $Pd(XH_3)(\eta^1\text{-}C_3H_5)(PH_3)_2$				
ΔE_2[b,d]	0.2	0.1	0.6	0.9
Pd	45.853	45.964	45.970	45.989
XH_3	9.244	17.068	35.062	52.996
$\eta^1\text{-}C_3H_5$	23.252	23.286	23.285	23.316
PH_3	17.826	17.865	17.861	17.871
PH_3	17.825	17.818	17.821	17.828

[a] The MP2/BS-II method. [b] The CCSD(T)/BS-II method (kcal/mol). [c] $\Delta E_1 = E_t[Pd(XH_3)(\eta^3\text{-}C_3H_5)(PH_3)] - E_t[Pd(XH_3)(\eta^1\text{-}C_3H_5)(PH_3)]$. [d] $\Delta E_2 = E_t[Pd(XH_3)(\eta^3\text{-}C_3H_5)(PH_3) + PH_3] - E_t[Pd(XH_3)(\eta^1\text{-}C_3H_5)(PH_3)_2]$.

Relative Stabilities of η^3- and η^1-Allyl Complexes. Optimized geometries of $Pd(CH_3)(\eta^1\text{-}C_3H_5)(PH_3)$ and $Pd(CH_3)(\eta^1\text{-}C_3H_5)(PH_3)_2$ are shown as examples in Chart 1. In the geometry optimization of $Pd(XH_3)(\eta^1\text{-}C_3H_5)(PH_3)$, the $Pd-C^1-C^2$ bond angle was taken to be the same as that of $Pd(XH_3)(\eta^1\text{-}C_3H_5)(PH_3)_2$, since $Pd(XH_3)(\eta^1\text{-}C_3H_5)(PH_3)$ spontaneously changed to $Pd(XH_3)(\eta^3\text{-}C_3H_5)(PH_3)$ in full geometry optimization. $Pd(XH_3)(\eta^1\text{-}C_3H_5)(PH_3)$ takes a T-shaped structure, because this is a three-coordinate d^8 complex.[44] The η^1-allyl form

(43) (a) Reed, A. E.; Curtiss, L. A.; Weinhold, F. *Chem. Rev.* **1988**, *88*, 849 and references therein. (b) The NBO populations of CH_3 and SiH_3 in $Pd(XH_3)(\eta^3\text{-}C_3H_5)(PH_3)$ depend little on the basis set of C and Si: 9.275e by the present basis set, 9.272e by 6-311G*,[43c] and 9.279e by 6-311+G*[43c,d] for X = C; 17.145e by the present basis set, 17.144e by 6-311G*, and 17.140e by 6-311+G* for X = Si. Moreover, the XH_3 population changes are almost the same in the present basis set, 6-311G*, and 6-311+G*; the decrease in the CH_3 population is 0.291e by the present basis set and 6-311G* and 0.303e by 6-311+G*, and that in the SiH_3 population is 0.532e by the present basis set, 0.531e by 6-311G*, and 0.526e by 6-311+G*. (c) Raghavachari, K.; Binkley, J. S.; Pople, J. A. *J. Chem. Phys.* **1980**, *72*, 650. (d) Clark, T.; Chandrasekhar, J.; Spitznagel, W. G.; Schleyer, P. v. R. *J. Comput. Chem.* **1983**, *4*, 294.

Downloaded by CARLI CONSORTIUM on June 30, 2009
Published on August 28, 1999 on http://pubs.acs.org | doi: 10.1021/om990296l

Chart 1

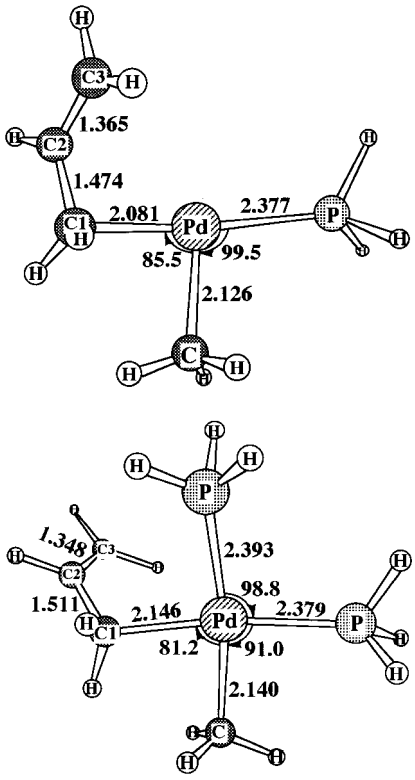

exhibits different features from the η^3-allyl form, as follows. (1) The Pd−PH_3 bond of the η^1-allyl form is much longer than that in the η^3-allyl form by 0.05−0.08 Å. This suggests that the *trans* influence of the η^1-allyl ligand is much stronger than that of the η^3-allyl ligand. (2) The Pd−XH_3 bond in the η^1-allyl form is much shorter than that of the η^3-allyl form, because the position *trans* to XH_3 is empty in the η^1-allyl form. (3) The Pd−C^1 bond of the η^1-allyl form is much shorter than that in the η^3-allyl form. This is probably because the η^1-allyl ligand must use only one C atom for the interaction with Pd but the η^3-allyl ligand can use two C atoms. The strong *trans* influence of the η^1-allyl ligand also arises from this feature.

$Pd(XH_3)(\eta^1\text{-}C_3H_5)(PH_3)$ is much less stable than the η^3-allyl form by about 7−8 kcal/mol, as shown in part B of Table 5. The electron populations of allyl and PH_3 ligands in the η^3-allyl form are greater than those of the η^1-allyl form, while the electron population of XH_3 is less in the η^1-allyl form than that in the η^3-allyl form. These electron populations suggest that the η^1-allyl ligand is less electron-donating than the η^3-allyl ligand. This is because the η^1-allyl ligand coordinates to Pd(II) with only one C atom but the η^3-allyl ligand coordinates with two C atoms, as discussed above. The smaller electron population of XH_3 indicates that XH_3 in $Pd(XH_3)(\eta^1\text{-}C_3H_5)(PH_3)$ can donate electrons to Pd(II) to a greater extent than in $Pd(XH_3)(\eta^3\text{-}C_3H_5)(PH_3)$. This is because the *trans* position of XH_3 is empty in $Pd(XH_3)(\eta^1\text{-}C_3H_5)(PH_3)$ and the η^1-allyl ligand is less electron-donating than the η^3-allyl ligand.

Now, we will discuss the relative stabilities of η^1-allyl and η^3-allyl forms when excess phosphine exists in the reaction medium. In this case, the T-shaped three-coordinate $Pd(XH_3)(\eta^1\text{-}C_3H_5)(PH_3)$ undergoes coordination of one additional PH_3 ligand to form a four-coordinate square-planar complex, $Pd(XH_3)(\eta^1\text{-}C_3H_5)(PH_3)_2$ (X = C, Si, Ge, Sn). This complex is slightly less stable than $Pd(XH_3)(\eta^3\text{-}C_3H_5)(PH_3) + PH_3$ by 0.2, 0.1, 0.6, and 0.9 kcal/mol for X = C, Si, Ge, and Sn, respectively (see part C of Table 5). This result indicates that the η^3-allyl to η^1-allyl transformation easily occurs in the presence of excess PH_3.

Reductive Elimination via the η^1-Allyl Form. When PH_3 exists in excess, $Pd(XH_3)(\eta^1\text{-}C_3H_5)(PH_3)_2$ would be formed, as discussed above. The reductive elimination from this complex was investigated with a model complex, $Pd(CH_3)_2(PH_3)_2$. As shown in Figure 4, the transition state is nonplanar, as reported.[45] The activation barrier was calculated to be 24.6 kcal/mol. On the basis of these results, we can estimate the energy change in the C−C reductive elimination via the η^1-allyl species, as follows: the energy destabilization of 0.2 kcal/mol occurs in the formation of $Pd(CH_3)(\eta^1\text{-}C_3H_5)(PH_3)_2$ from $Pd(CH_3)(\eta^3\text{-}C_3H_5)(PH_3) + PH_3$, and in addition, the C−C reductive elimination of $Pd(CH_3)(\eta^1\text{-}C_3H_5)(PH_3)_2$ needs an activation energy of 24.6 kcal/mol which is calculated for the model, $Pd(CH_3)_2(PH_3)_2$.[46] This means that the TS of the C−C reductive elimination of $Pd(CH_3)(\eta^1\text{-}C_3H_5)(PH_3)_2$ is about 24.8 kcal/mol (=0.2 + 24.6) higher in energy than $Pd(CH_3)(\eta^3\text{-}C_3H_5)(PH_3) + PH_3$, which is almost the same as the E_a value of the C−C reductive elimination starting from $Pd(CH_3)(\eta^3\text{-}C_3H_5)(PH_3)$. Thus, the reductive elimination via $Pd(CH_3)(\eta^1\text{-}C_3H_5)(PH_3)_2$ cannot be excluded, when PH_3 exists in excess.

Now, we will investigate whether the reductive elimination proceeds through the η^1-allyl form when PH_3 does not exist in excess. In the C−C reductive elimination via the η^1-allyl form, $Pd(CH_3)(\eta^3\text{-}C_3H_5)(PH_3)$ must convert to $Pd(CH_3)(\eta^1\text{-}C_3H_5)(PH_3)$, and then, $Pd(CH_3)(\eta^1\text{-}C_3H_5)(PH_3)$ undergoes the C−C reductive elimination, as shown in Scheme 3. This reductive elimination of $Pd(CH_3)(\eta^1\text{-}C_3H_5)(PH_3)$ was investigated here with a model complex, $Pd(CH_3)_2(PH_3)$, since the TS of this C−C reductive elimination is considered similar to that of $Pd(CH_3)(\eta^1\text{-}C_3H_5)(PH_3)$.[47] The geometry changes are shown in Figure 4. The activation barrier of 11.7 kcal/mol is much lower than that of $Pd(CH_3)_2(PH_3)_2$, probably because the geometry of the $Pd(PH_3)$ moiety changes little in the C−C reductive elimination of $Pd(CH_3)_2(PH_3)$ but the P−Pd−P angle of the $Pd(PH_3)_2$ moiety considerably decreases in the C−C reductive elimination of $Pd(CH_3)_2(PH_3)_2$.[48] The formation of $Pd(CH_3)(\eta^1\text{-}C_3H_5)(PH_3)$ from $Pd(CH_3)(\eta^3\text{-}C_3H_5)(PH_3)$ requires the considerable

(44) Komiya, S.; Albright, T. A.; Hoffmann, R.; Kochi, J. K. *J. Am. Chem. Soc.* **1976**, *98*, 7255.

(45) Sakaki, S.; Mizoe, N.; Musashi, Y.; Biswas, B.; Sugimoto, M. *J. Phys. Chem.* **1937**, *41*, 8027.

(46) A more simple discussion could be presented if we were able to successfully optimize the TS structure of the C−C reductive elimination of $Pd(CH_3)(\eta^1\text{-}C_3H_5)(PH_3)_2$. However, we failed to optimize it because of the significant flexibility of the η^1-C_3H_5 moiety. The discussion presented here seems useful for the comparison of the reductive elimination of $Pd(CH_3)(\eta^1\text{-}C_3H_5)(PH_3)_2$ with that of $Pd(CH_3)(\eta^3\text{-}C_3H_5)(PH_3)$.

(47) Since the C^2═C^3 bond weakly coordinates with Pd at the TS (see **TS-C**, **TS-Si**, **TS-Ge**, and **TS-Sn** in Figures 1 and 2), the C−C reductive elimination of $Pd(CH_3)_2(PH_3)$ might be considered a reasonable model of the reductive elimination of $Pd(CH_3)(\eta^1\text{-}C_3H_5)(PH_3)$.

(48) A similar discussion was previously presented for the Si−H oxidative addition to $RhCl(PH_3)_2$ and $RhCl(CO)(PH_3)_2$: Sakaki, S.; Ujino, Y.; Sugimoto, M. *Bull. Chem. Soc. Jpn.* **1996**, *69*, 3047.

Downloaded by CARLI CONSORTIUM on June 30, 2009
Published on August 28, 1999 on http://pubs.acs.org | doi: 10.1021/om990296l

Downloaded by CARLI CONSORTIUM on June 30, 2009
Published on August 28, 1999 on http://pubs.acs.org | doi: 10.1021/om990296l

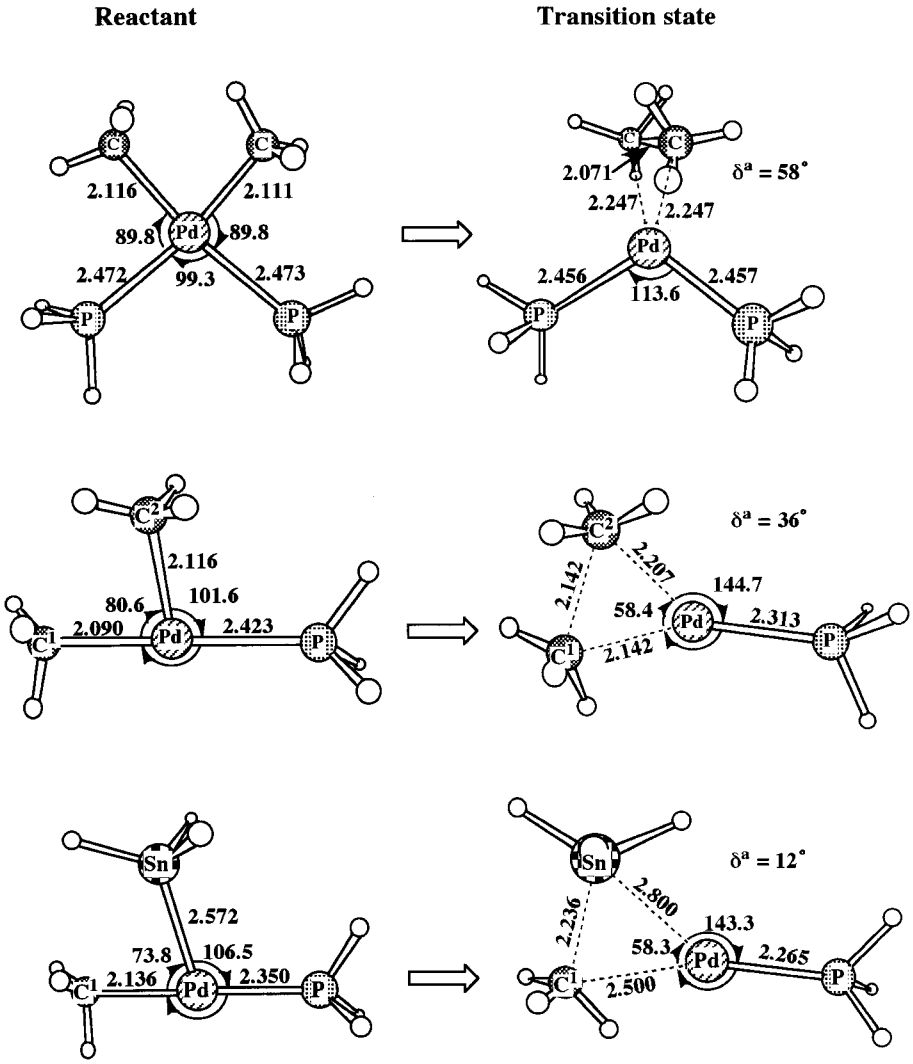

Figure 4. Geometry changes in the C−C reductive elimination of $Pd(CH_3)_2(PH_3)_2$ and the C−X reductive elimination of $Pd(CH_3)(XH_3)(PH_3)$ (X = C, Sn). Bond lengths are in Å, and bond angles are in deg. The δ value indicates the dihedral angle between the P−Pd−P and Pd−C−C planes in $Pd(CH_3)_2(PH_3)_2$ and that between the Pd−C^1−X and P−Pd−C^1 planes in $Pd(CH_3)(XH_3)(PH_3)$.

Scheme 3

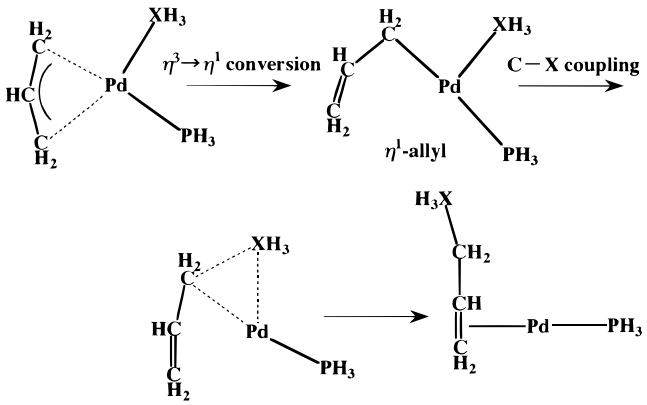

destabilization energy of 8.6 kcal/mol (see above and Table 5B), and in addition, the C−C reductive elimination of $Pd(CH_3)(\eta^1\text{-}C_3H_5)(PH_3)$ needs the activation energy of 11.7 kcal/mol which is calculated for the model $Pd(CH_3)_2(PH_3)$. Thus, the TS of the C−C reductive elimination via $Pd(CH_3)(\eta^1\text{-}C_3H_5)(PH_3)$ is estimated to be less stable in energy than $Pd(CH_3)(\eta^3\text{-}C_3H_5)(PH_3)$ by 20.3 kcal/mol (=8.6 + 11.7), which is almost the same as the E_a value of the spontaneous C−C reductive elimination directly starting from $Pd(CH_3)(\eta^3\text{-}C_3H_5)(PH_3)$. Also, if the C−Sn reductive elimination occurs via $Pd(SnH_3)(\eta^1\text{-}C_3H_5)(PH_3)$, $Pd(SnH_3)(\eta^3\text{-}C_3H_5)(PH_3)$ must convert to the η^1-allyl form and then the C−Sn reductive elimination occurs. The C−Sn reductive elimination via the η^1-allyl form requires a destabilization energy of 7.8 kcal/mol for the conversion of the η^3-allyl form to the η^1-allyl form (see part B of Table 5) and in addition the activation barrier of 4.2 kcal/mol for the C−Sn reductive elimination of $Pd(SnH_3)(\eta^1\text{-}C_3H_5)(PH_3)$ which is calculated for a model, $Pd(CH_3)(SnH_3)(PH_3)$. Thus, the sum of these energies corresponds to the barrier height of the C−Sn reductive elimination via the η^1-allyl species. Again, this value 12.0 kcal/mol (=7.8 + 4.2) is almost the same as the activation barrier of the spontaneous C−Sn reductive elimination of $Pd(SnH_3)(\eta^3\text{-}C_3H_5)(PH_3)$. From these results, it cannot be determined whether the spontaneous reductive elimination of the η^3-allyl form takes place more favorably than does the reductive elimination via the η^1-allyl form.

To clarify the reaction course, we performed the intrinsic reaction coordinate (IRC) calculation[49] of the

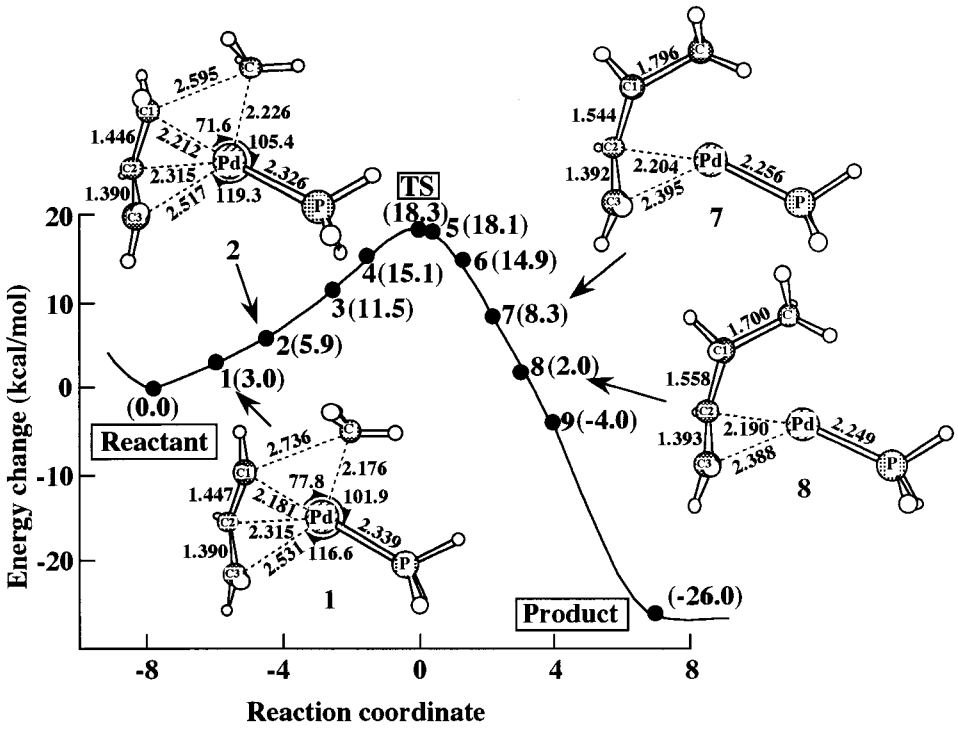

Figure 5. Energy change and geometry change calculated by IRC calculation of the C−C reductive elimination of Pd(CH$_3$)(η^3-C$_3$H$_5$)(PH$_3$). The energy zero was taken for the reactant, and IRC calculation was carried out with the MP2/BS-I method.

Downloaded by CARLI CONSORTIUM on June 30, 2009
Published on August 28, 1999 on http://pubs.acs.org | doi: 10.1021/om990296l

C−C reductive elimination of Pd(CH$_3$)(η^3-C$_3$H$_5$)(PH$_3$). If the η^3-allyl form changes first to the η^1-allyl form and then the C−C bond formation occurs, as shown in Scheme 3, the reaction should be considered to take place via the η^1-allyl form. However, if the η^3-allyl form gradually changes to the η^1-allyl form of **TS-C** as the CH$_3$ group approaches the allyl group, the reaction should be considered to take place directly from the η^3-allyl form. As clearly shown in Figure 5, the η^1-allyl form cannot be observed in the reactant side, and the geometry of the η^3-allyl form gradually changes to the η^1-allyl form in a concerted manner with the approach of CH$_3$ to allyl. From these geometry changes, it should be clearly concluded that the C−C reductive elimination directly starts from the η^3-allyl complex without the η^3-allyl to η^1-allyl conversion.

Comparison between the C−X Reductive Eliminations of CH$_3$−XH$_3$ and (η^3-C$_3$H$_5$)−XH$_3$ (X = C, Sn). It is interesting to make a comparison between the reductive eliminations of η^3-allyl and η^1-alkyl groups. Here, we selected X = C, Sn since they are considered two extreme cases. The C−C reductive elimination of Pd(CH$_3$)(η^3-C$_3$H$_5$)(PH$_3$) requires a considerably large E_a value of 23.3 kcal/mol (vide supra). On the other hand, that of Pd(CH$_3$)$_2$(PH$_3$) needs a moderate E_a value of 11.7 kcal/mol. A similar difference is observed in the C−Sn reductive elimination; the E_a value is 11.5 kcal/mol in Pd(SnH$_3$)(η^3-C$_3$H$_5$)(PH$_3$) and 4.2 kcal/mol in Pd(CH$_3$)(SnH$_3$)(PH$_3$). These results clearly indicate that the C−X reductive elimination of the η^3-allyl group occurs much less easily than that of the η^1-alkyl group.

The larger E_a value of Pd(XH$_3$)(η^3-C$_3$H$_5$)(PH$_3$) is interpreted in terms of the Pd−CH$_3$ and Pd−(η^3-C$_3$H$_5$) bond energies. The Pd−CH$_3$ bond energy is estimated to be 26.3 kcal/mol (Table 3). Considering eq 11, we can estimate the Pd−(η^3-C$_3$H$_5$) bond energy with eq 12. In

$$\mathrm{Pd(CH_3)(\eta^3\text{-}C_3H_5)(PH_3)} \rightarrow \mathrm{Pd(PH_3) + CH_2{=}CHCH_2CH_3} \quad (11)$$

$$E[\mathrm{Pd}(\eta^3\text{-}\mathrm{C_3H_5})] = \Delta E(\text{eq 11}) - E(\mathrm{Pd{-}CH_3}) + E(\mathrm{C_3H_5{-}CH_3}) \quad (12)$$

$$\mathrm{CH_2{=}CHCH_2CH_3} \rightarrow \mathrm{CH_2{=}CHCH_2^{\bullet} + {}^{\bullet}CH_3} \quad (13)$$

eq 12, ΔE(eq 11) is the reaction energy of eq 11, and E(Pd−CH$_3$) and E(C$_3$H$_5$−CH$_3$) are Pd−CH$_3$ and C$_3$H$_5$−CH$_3$ bond energies, respectively. E(C$_3$H$_5$−CH$_3$) is calculated to be 79.2 kcal/mol with eq 13, and ΔE(eq 11) is −1.9 kcal/mol. Using these values, the E[Pd−(η^3-C$_3$H$_5$)] value is estimated to be 50.8 kcal/mol. Since the Pd−(η^3-C$_3$H$_5$) bond is much stronger than the Pd−CH$_3$ bond energy, the C−X reductive eliminations of the η^3-allyl ligand require a much higher activation energy than that of the alkyl ligand. It is not unreasonable that the difference between Pd−CH$_3$ and Pd−(η^3-C$_3$H$_5$) bond energies is much greater than the difference in E_a between the C−X reductive eliminations of η^3-allyl and η^1-alkyl ligands, because the Pd−(η^3-C$_3$H$_5$) and Pd−CH$_3$ bonds are not completely broken at the transition state.

We will mention here a comparison between alkyl−alkyl and alkyl−stannyl reductive eliminations. In the TS of Pd(CH$_3$)$_2$(PH$_3$), the Pd−CH$_3$ bonds lengthen by 0.09 and 0.05 Å (Figure 4), suggesting that the Pd−CH$_3$ bonds are not weakened very much, while the C−C distance is 2.14 Å, indicating that the C−C bond is not sufficiently formed yet. In the TS of Pd(CH$_3$)(SnH$_3$)(PH$_3$), the Pd−SnH$_3$ and Pd−CH$_3$ bonds lengthen by 0.23 and 0.36 Å, respectively (Figure 4). Though the Pd−

(49) Fukui, K. *Acc. Chem. Res.* **1981**, *14*, 363.

CH_3 bond is somewhat weakened, the Pd−SnH_3 bond lengthening is about 8% of the equilibrium Pd−SnH_3 bond in Pd(CH_3)(SnH_3)(PH_3), indicating that the Pd−SnH_3 bond still exists in the transition state. The C−Sn distance is only 0.07 Å longer than that of the product, indicating that the C−Sn bond is already formed. From these features, it is again clearly concluded that the Sn atom can form the C−Sn bond without the Pd−Sn bond breaking, because of the hypervalency of Sn. In the TS of Pd(CH_3)$_2$(PH_3), the C−C bond is not formed and the Pd−CH_3 bond still exists, which results from no hypervalency of C.

Conclusions

The geometries, bonding nature, and reactivities in the C−X reductive elimination of Pd(XH_3)(η^3-C_3H_5)(PH_3) (X = C, Si, Ge, Sn) were theoretically investigated with MP2-MP4(SDQ) and CCSD(T) methods. Several interesting geometrical features are observed in Pd(XH_3)(η^3-C_3H_5)(PH_3), as follows. (1) The Pd−C^3 bond positioned *trans* to XH_3 is longer than the Pd−C^1 bond positioned *trans* to PH_3 because CH_3, SiH_3, GeH_3, and SnH_3 exhibit stronger *trans* influence than PH_3. (2) Since the Pd−C^3 bond becomes longer in the order CH_3 < GeH_3 < SnH_3 ≈ SiH_3, which indicates that the *trans* influence of group 14 elements increases in the order CH_3 ≪ GeH_3 < SnH_3 ≈ SiH_3. (3) The C^1−C^2 and C^2−C^3 bond distances are calculated to be 1.443−1.452 and 1.395−1.400Å, respectively, which indicates that the η^3-allyl group slightly distorts toward an η^1-allyl structure.

The transition state of the C−C reductive elimination is much different from those of the other reductive eliminations. In the former, the Pd−CH_3 bond lengthens greatly, while the C−C distance between allyl and CH_3 is still considerably long. In the other transition states, on the other hand, the Pd−XH_3 bond moderately lengthens and the C−X bond between allyl and XH_3 is about 80% formed. These features suggest that the C−X bond formation occurs without the Pd−XH_3 bond breaking in these transition states. This is because Si, Ge, and Sn elements have hypervalency.

The C−C reductive elimination of Pd(CH_3)(η^3-C_3H_5)(PH_3) is considerably exothermic (E_{exo} = 27.7 kcal/mol) and requires a high activation energy (E_a = 23.3 kcal/mol). The C−Si and C−Ge reductive eliminations of Pd(SiH_3)(η^3-C_3H_5)(PH_3) and Pd(GeH_3)(η^3-C_3H_5)(PH_3) occur with moderate E_a values of 11.6 and 12.8 kcal/mol, respectively, and small exothermicities of 6.0 and 1.6 kcal/mol, respectively. On the other hand, the C−Sn reductive elimination of Pd(SnH_3)(η^3-C_3H_5)(PH_3) is slightly endothermic (5.9 kcal/mol) and requires almost the same E_a value (11.5 kcal/mol) as those of C−Si and C−Ge reductive eliminations. The highest activation barrier of the C−C reductive elimination can be explained in terms of the large destabilization energy caused by the direction change of CH_3, which results from the absence of hypervalency of the C atom.

The significant exothermicity of the C−C reductive elimination reaction can be explained in terms of C−XH_3 and Pd−XH_3 bond energies. The C−XH_3 bond energy increases in the order E(C−Sn) < E(C−Ge) < E(C−Si) < E(C−C), and the Pd−XH_3 bond energy increases in the order E(Pd−CH_3) ≪ E(Pd−SnH_3) < E(Pd−GeH_3) < E(Pd−SiH_3). Since the weakest Pd−CH_3 bond is broken and the strongest C−C bond is formed in the C−C reductive elimination, this reaction is the most exothermic. The C−Si and C−Ge reductive eliminations are moderately exothermic and the C−Sn reductive elimination is moderately endothermic, since the weaker C−Si, C−Ge, and C−Sn bonds are formed and the weaker Pd−SiH_3, Pd−GeH_3, and Pd−SnH_3 bonds are broken in these reactions.

The relative stabilities of η^3-allyl and η^1-allyl complexes were investigated. Pd(XH_3)(η^1-C_3H_5)(PH_3) is much less stable than the η^3-allyl form by about 8.0 kcal/mol. If excess PH_3 exists in the reaction medium, Pd(XH_3)(η^1-C_3H_5)(PH_3) undergoes additional coordination of PH_3 to form a four-coordinate square-planar complex, Pd(XH_3)(η^1-C_3H_5)(PH_3)$_2$. Since the energy difference between Pd(XH_3)(η^1-C_3H_5)(PH_3)$_2$ and Pd(XH_3)(η^3-C_3H_5)(PH_3) + PH_3 is very small (0.2−0.9 kcal/mol), Pd(XH_3)(η^1-C_3H_5)(PH_3)$_2$ might be formed. The C−C reductive elimination of Pd(CH_3)$_2$(PH_3)$_2$ occurs with an E_a value of 24.6 kcal/mol, which is similar to the E_a value of the C−C reductive elimination of Pd(CH_3)(η^3-C_3H_5)(PH_3). Thus, the C−C reductive elimination via Pd(CH_3)(η^1-C_3H_5)(PH_3)$_2$ cannot be excluded when PH_3 exists in excess. The IRC calculation clearly shows that Pd(CH_3)(η^1-C_3H_5)(PH_3) does not exist in the reaction course of the C−C reductive elimination of Pd(CH_3)(η^3-C_3H_5)(PH_3). Thus, it should be concluded that the C−C reductive elimination of Pd(CH_3)(η^3-C_3H_5)(PH_3) spontaneously takes place from the η^3-allyl species without conversion to the η^1-allyl species when PH_3 does not exist in excess.

Interestingly, the (η^3-C_3H_5)−XH_3 reductive elimination needs a much larger E_a value than the CH_3−XH_3 reductive elimination. This result is interpreted in terms of the Pd−(η^3-C_3H_5) bond being much stronger than the Pd−CH_3 bond.

Acknowledgment. Computations were carried out with an IBM SP2 machine at the Institute for Molecular Science (Okazaki, Japan) and an IBM RS6000/3CT workstation in our laboratory. B.B. thanks the Ministry of Education, Science, Sports, and Culture of Japan for a scholarship. This work was financially supported by Grants-in-Aid for Scientific Research on Priority Areas "The Chemistry of Inter-Element Linkage" (No. 09239104) and "Molecular Physical Chemistry" (No. 111662533) from the Ministry of Education, Science, Sports, and Culture.

Supporting Information Available: Figures giving the energy changes by the rotation of the −CH_2CX_3 group in Pd(PH_3)(CH_2=$CHCH_2XH_3$) (X = C, Si), vibrational frequency analysis, population changes of C−Ge and C−Sn reductive eliminations, and optimized geometries of η^1-allyl complexes. This material is available free of charge via the Internet at http://pubs.acs.org.

OM990296L

Downloaded by CARLI CONSORTIUM on June 30, 2009
Published on August 28, 1999 on http://pubs.acs.org | doi: 10.1021/om990296l